(Article begins on next page)

17 April 2024

Taylor & Francis
Taylor & Francis Group

Percolation transition in water–AOT–decane microemulsion investigated by transient grating measurement

C. ZIPARO*†‡, R. ERAMO†§, C. M. C. GAMBI§‡, and R. TORRE†‡§

†European Laboratory for Non-Linear Spectroscopy (LENS), Università di Firenze, Via N. Carrara 1, I-50019 Sesto Fiorentino, Firenze, Italy
‡INFM-CRS-Soft Matter (CNR), c/o Università la Sapienza Piaz. A. Moro 2, I-00185, Roma, Italy
§Dipartimento di Fisica, Università di Firenze, Via Sansone 1, I-50019 Sesto Fiorentino, Firenze, Italy

We report results from a heterodyne-detected transient grating experiment on a three-component microemulsion system, consisting of water–AOT–decane. We studied the microemulsion characterized by a water-to-AOT ratio of $X = 40.8$ and a volume fraction $\phi = 0.50$, in a temperature range around the percolation threshold. The measurements have been performed with two exchanged momenta $q \approx 1$ and $2\,\mu m^{-1}$, corresponding to sound frequencies around 200 and 420 MHz. The measured sound velocities show small but significant evidence of the percolation transition in the temperature domain.

1. Introduction

Microemulsions [1–17] are transparent, optically homogeneous and thermodynamically stable systems composed by a mixture of oil, water and surfactant. Water-in-oil microemulsions are made by water droplets coated by a surfactant monolayer dispersed in a bath of oil.

The microemulsion investigated here is the widely studied system water–AOT–decane, where AOT (sodium di-2-ethylhexylsulfosuccinate) is the ionic surfactant, having a polar hydrophilic head and two hydrocarbon hydrophobic tails. In the absence of water, the hydrophilic heads of AOT aggregate together to avoid the oil phase, the resulting spherical micelles consisting of ≈ 22 molecules, with a radius of ≈ 1.5 nm. When water is added, it is included into the micelles, swelling them and forming droplets with water cores having a diameter determined by the molar ratio $X = [\text{water}]/[\text{AOT}]$. Provided this ratio is held fixed, the volume fraction of the

---

*Corresponding author. Email: ziparo@lens.unifi.it

dispersed phase $\phi = (V_w + V_{AOT})/V_{tot}$, defined by the ratio between the water-plus-surfactant and total volumes, can be varied without changing the droplet size. The ϕ–T phase diagram of the system for a molar ratio $X = 40.8$ is reported in [2, 10 ,11] and shows a single-phase lower temperature L_2 region and a two-phase region at high temperature, at higher temperatures and $\phi \geq 0.4$, other morphological phases can be observed. The phase region here investigated is the single-phase L_2, where the droplet water core has an average radius of around 5 nm, and a percolation transition has been observed by low-frequency electrical conductivity measurements [2, 18], by dielectric spectroscopy [1] by differential scanning calorimetry [19]. For what concerns sound propagation, extensive experiments on AOT-based systems have been performed with ultrasonic techniques [1, 3] and Brillouin scattering [1, 4, 5]. In the Brillouin hypersonic frequency range ($f \approx 5$ GHz) the percolation transition as a function of temperature has been detected for dense systems ($\phi \geq 0.5$) as a small change of the slope of the velocity curve and a bump in the absorption curve [1]. In [4] a bump at the thermal threshold is reported in the sound velocity as a function of temperature. To our knowledge, in the ultrasonic domain investigated here no effect has been observed [1, 3].

The heterodyne detected transient grating measurements presented here show that a small, but significant, effect of the percolation transition on the sound velocity can indeed be observed in the temperature domain also for sound frequency as low as 200 MHz.

2. Experiment

We used AOT from Fluka (purity 99%) repurified before use as in [20] and n-decane oil ($C_{10}H_{22}$) from Sigma (purity 99%). Water was cleaned from a Millipore Milli-Q system. The volume fraction ϕ is determined from the volume's ratio. The components are added by weight and then converted to volume using the bulk densities (AOT 1.13 g/cm^3, decane 0.73 g/cm^3). We chose to work with the widely studied molar ratio $X = 40.8$, with a volume fraction $\phi = 0.50$, corresponding to a quite dense microemulsion system which has a percolation temperature around 25°C [18].

In a transient grating (TG) experiment [21–23] the sample excitation is produced by two high-power laser pulses, of wavelength λ_p, obtained by dividing a single pulsed laser beam, interfering and producing an impulsive, spatially periodic variation of the dielectric constant, $\delta\epsilon(\mathbf{r}, t)$, inside the sample. This relaxing excitation is probed by a continuous wave laser beam, typically of a different wavelength λ_s. This beam impinges on the induced grating at the Bragg angle producing a diffracted beam, spatially separated by the pump and the probe beams. This diffracted beam is the signal measured in the experiment, yielding the dynamic information from the relaxing grating. Optical heterodyne detection (HD) is used to measure this weak scattered field by mixing it with a second CW laser beam, coherent with the probe beam. The resulting heterodyne signal is proportional to the spatial Fourier component of the dielectric constant

$$S(t) \propto \delta\epsilon(q, t) \tag{1}$$

where $q = 2k \sin \theta$ is the grating wavevector, with $k = 2\pi/\lambda_p$ and 2θ the angle between the two wavevectors of the pump beams.

The experimental details concerning the laser and the optical set-up are extensively reported in [21]; here we recall only the main features in order to make clear the present experimental conditions. The excitation is produced by two infrared pulses, with $\lambda_p = 1064$ nm wavelength, 20 ps duration, 100 μJ energy with a repetition rate of 10 Hz. The pulses are generated by an amplified laser system (Ekspla, mod. PL2143A) consisting of a passively mode-locked Nd-YAG laser with integrated regenerative amplification, followed by an Nd-YAG flash pumped double-pass amplifier. The probing beam, with $\lambda_s = 532$ nm and an averaged power after chopping ≈ 20 mW, is produced by a diode-pumped intracavity-doubled Nd-YVO (Verdi-Coherent); this is a CW single-mode laser characterized by excellent intensity stability with low and flat noise-intensity spectrum. The beam intensities and polarizations are controlled by half-wave plates and polarizers. We used a phase grating as a diffractive optical element (DOE) made by Edinburgh Microoptics to diffract both laser fields. The excitation grating induced in the sample is the mirror image of the enlightened DOE phase pattern and has an extension in the q direction of ≈ 5 mm; the probing beam is focused in a circular spot ≈ 0.5 mm in diameter. The use of a DOE substantially improves the TG experiments [21, 24, 25]. The HD-TG signal, after optical filtering, is measured by an 800 MHz bandwidth avalanche photodiode and recorded by a Tektronix oscilloscope with a bandwidth of 7 GHz and a sampling rate of 20 Gs/s. The signal is averaged over many pump pulses (usually 3000 pulses) in the time range 0–1 ms.

3. Results

We made measurements for the two nominal values $q = 1$ and $2\,\mu m^{-1}$ of the exchanged momentum. To measure accurately the exchanged momentum a preliminary q calibration procedure was done, making a few test measurements on a distilled water sample (a phial from Galenica Senese), as reported in figure 1 for $q = 1\,\mu m^{-1}$. To overcome the uncertainty due to the temperature measurement with different sample holders, the calibration measurements were performed on a large temperature interval, where water shows its characteristic maximum around 80°C in the sound velocity versus temperature curve. By comparing the measured sound velocity with the literature data [26, 27] the following values of q were obtained: $q = (0.9974 \pm 0.0005)\,\mu m^{-1}$, and $q = (2.090 \pm 0.001)\,\mu m^{-1}$.

In figure 2 a typical transient grating heterodyne spectrum is shown. In the same figure a fit is superimposed on the experimental data. As can be seen from the residuals curve (fit minus data) the fit is quite satisfactory. The fitting function is obtained by convolving the experimentally measured set-up resolution function, with a width around 1 ns FWHM, with the function

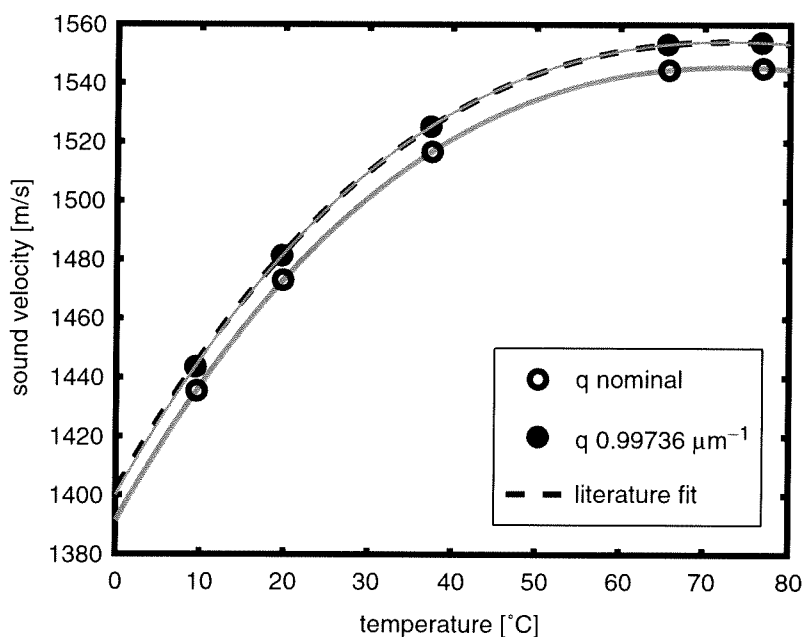$$S = [A \cos \omega_s t + B \sin \omega_s t]e^{-t/\tau_s} + Ce^{-t/\tau_t} \qquad (2)$$

Figure 1.   Calibration of q for $q = 1\,\mu m^{-1}$. The water velocity data at $q = 1\,\mu m^{-1}$ nominal (empty circles) was fitted by a cubic polynomial by comparing this fit with a cubic polynomial fit of the literature data; a value $q = (0.9974 \pm 0.0005)\,\mu m^{-1}$ was obtained. An analogous procedure was followed for $q = 2\,\mu m^{-1}$.
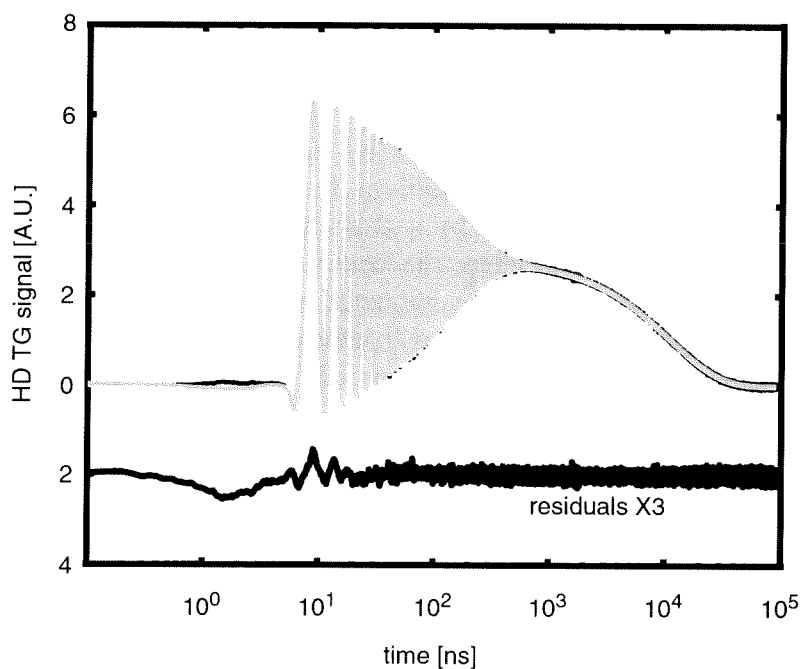

Figure 2.   HD-TG signal of the microemulsion sample. A fit (grey line) is superimposed to the experimental points (dots). Shifted and multiplied by 3 for clarity, a plot (black line) of the fit residuals is also shown in the figure. The temperature is 22.5°C, around 2.5 degrees below the thermal percolation threshold.

where $\omega_s = v_s q$ is the sound frequency, v_s being the sound velocity, $\tau_s = 1/\Gamma_B = 1/\alpha v_s$ is the sound decay time, with $\alpha/f^2 = 4\pi^2\Gamma_B/q^2 v_s^3$ the sound absorption coefficient, Γ_B the Brillouin ω-linewidth HWHM and τ_t is the thermal decay time. Assuming that the sample dielectric constant is a function of the density [28], i.e. neglecting its temperature dependence, we have $A = -C$; if there is no electrostrictive effect, i.e. we have a purely thermal grating, $B = 0$, and the signal remains of the same sign during the whole temporal range. For our sample the spectrum is the result of both a thermal and an electrostrictive grating, as can be seen by the oscillatory sound response region, where the signal passes through the baseline. An analogous electrostrictive signature is also visible in the pure decane sample.

In figure 3 we report the sound velocities and the sound absorption coefficients of the microemulsion obtained by fitting our data, as a function of temperature. Our measurements are in good agreement with ultrasonic literature data, measured at 25 MHz and taken from [1]. If we use as reference a linear fit to the data below the percolation temperature, $T_p \approx 25°C$, we can observe crossing the threshold a small but significant discrepancy for both frequencies. A similar finding was found in [1], but only for the high-frequency Brillouin measurement (5 GHz) and for the higher density ($\phi = 0.75$) microemulsion. A more quantitative analysis can be made by comparing the χ^2 values for a fit made with a single line to the whole temperature range or with a broken line, changing the slope at T_p. The figures for the $q = 1\,\mu m^{-1}$ measurement are reported in the table 1. Estimating a value ≈ 1 m/s for the standard deviation of the velocity data, the reduced χ^2 results in ≈ 1.7 for the single-line fit, while $\chi^2 \approx 0.8$ for the broken-line case. Similar results are obtained in the $q = 2\,\mu m^{-1}$ measurement, thus confirming that the bending of the velocity curve is a clearly observed effect.

An alternative view can be obtained by calculating the elastic modulus of the droplets following the effective medium theory [5, 6]. In this approach the microemulsion is seen as composed by a continuum oil phase, of complex elastic modulus $\beta_o = \varrho_o v_o^2[1 + i\alpha_o\lambda/\pi]$, where the water–AOT droplets of elastic modulus $\beta_d = \beta_d' + i\beta_d''$ are dispersed. We have indicated with ϱ_o the density, v_o the sound velocity, and α_o the sound absorption coefficient of the oil, and with λ the sound wavelength. The β_d modulus is calculated from the experimentally measured microemulsion modulus β and from β_o by Wood's formula:

$$\frac{1}{\beta} = \frac{\phi}{\beta_d} + \frac{1-\phi}{\beta_o} \qquad (4)$$

with $\beta = \varrho v^2[1 + i\alpha\lambda/\pi]$, where $\varrho = \phi\varrho_d + (1 - \phi)\varrho_o$ is the density, v the sound velocity, and α the sound absorption coefficient of the microemulsion. In figure 4 we report our measurement of the oil parameters. In figure 5 the real and imaginary parts of the elastic modulus of the droplets are shown for both q values; the quadratic fit superimposed on the real part has a maximum slightly below 25°C, the percolative temperature observed in the static conductivity measurements [3]. The percolation effect in the effective medium approach gives an enhancement $\approx 1\%$ of the real part of the elastic modulus, slightly over the measurement error.
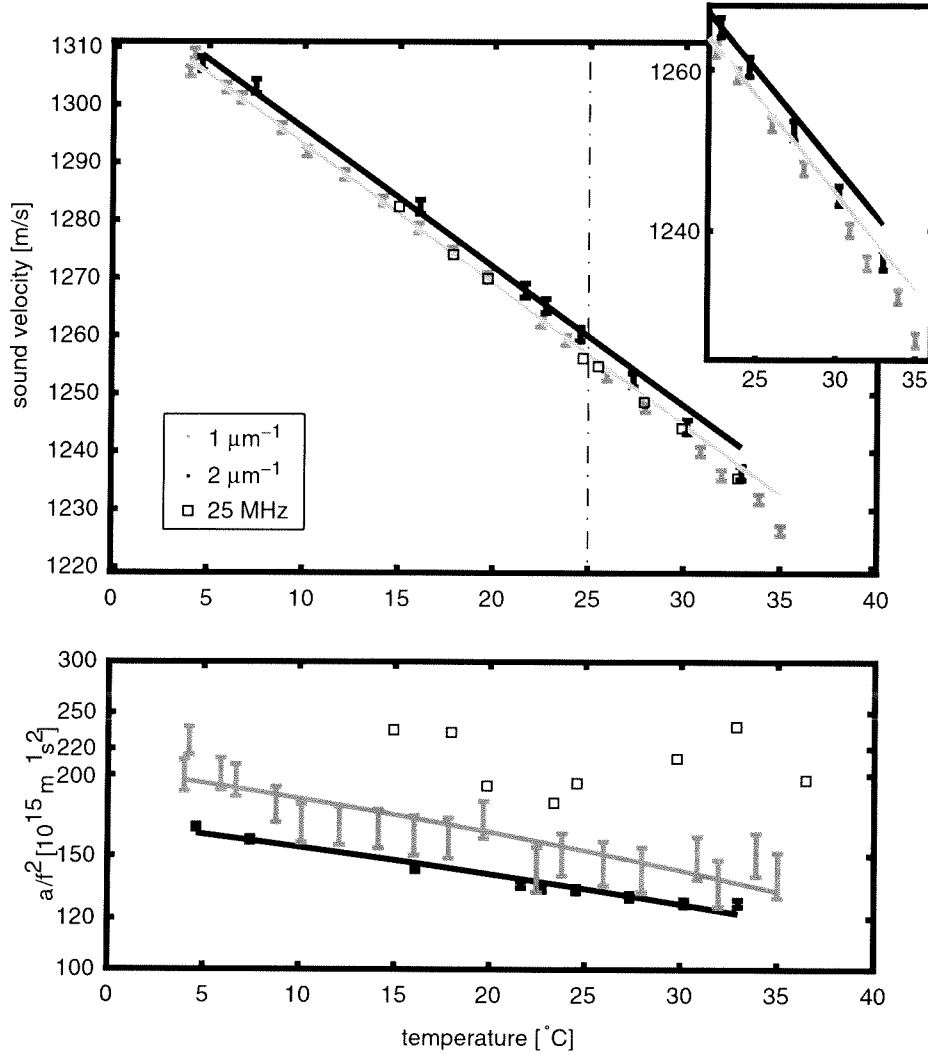
Figure 3. Microemulsion sound velocity and absorption versus temperature. Our measurements correspond to sound frequencies around 200 MHz ($q = 1\,\mu m^{-1}$) and 420 MHz ($q = 2\,\mu m^{-1}$) and are compared with ultrasonic data measured at 25 MHz from [1]. The lines are linear fits to the data below the percolation threshold, $T_p \approx 25°C$. A small but significant discrepancy from the linear trend (inset) is visible for both frequencies crossing the percolation threshold in the sound velocity results.

Table 1. Statistical analysis for the $q = 1\,\mu m^{-1}$ case. The sum of residuals $\Sigma = (y - y_{fit})^2$ and the degree of freedom n are reported for three cases: (i) Line fit to data points with temperatures below $T_p = 25°$ C; (ii) a broken line (i.e. a line changing slope at $T = T_p$) fitted to the whole T-range; (iii) single-line fitted to the whole range. The broken line fit gives a $\chi^2/n \approx 0.8$ on the whole temperature range, while the single-line fit has $\chi^2/n \approx 1.7$, thus confirming that the bending of the velocity curve is clearly observed. Similar figures, $\chi^2/n \approx 1$ (broken line) and $\chi^2/n \approx 2$ (single line), are obtained for the $q = 2\,\mu m^{-1}$ case.

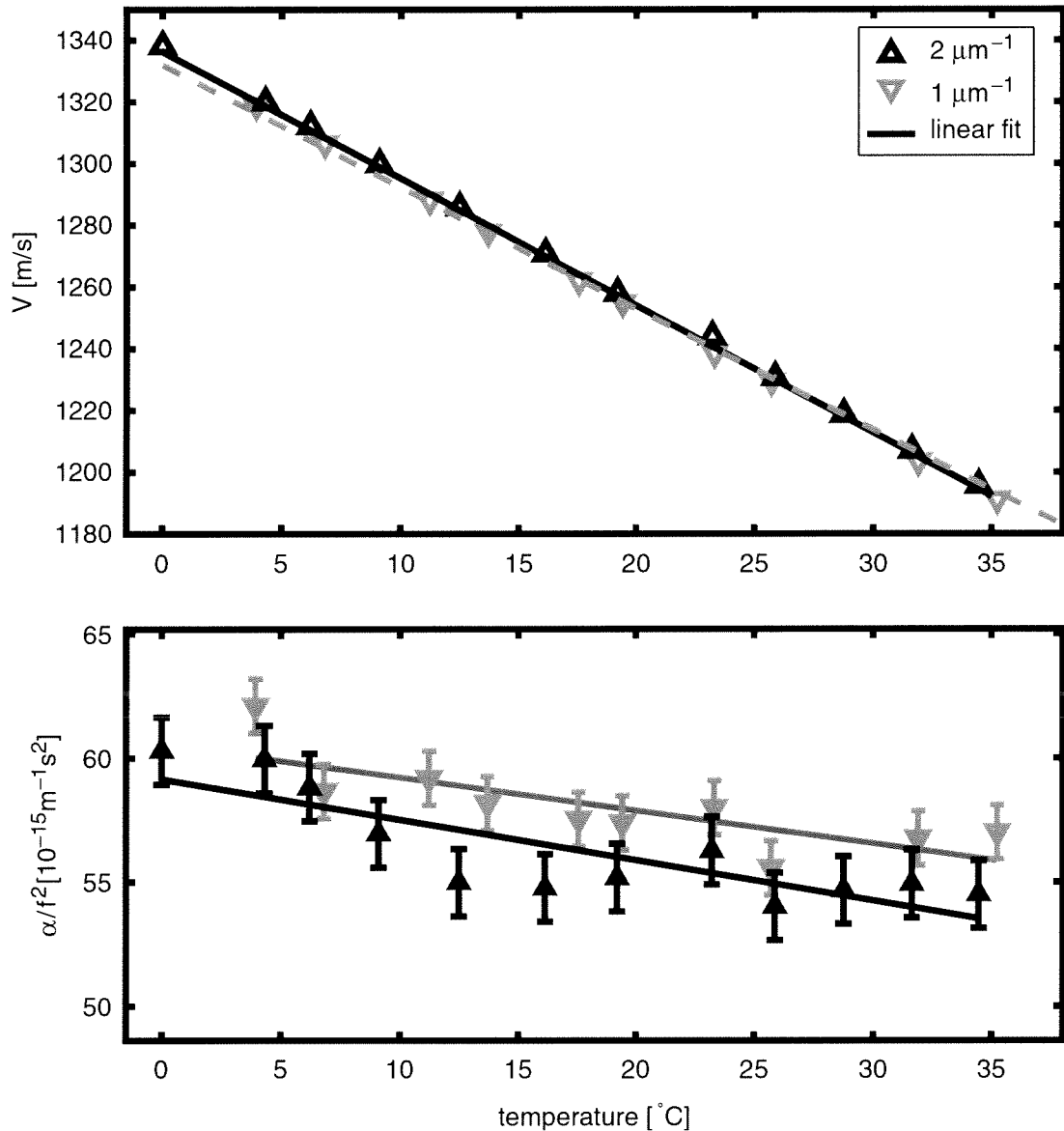| Fit range	Σ	n	Σ/n
below T_p (single-line)	8.52	11	0.774
whole (broken-line)	11.58	15	0.772
whole (single-line)	29.24	17	1.72

Figure 4. Decane sound velocity and absorption coefficient α/f^2 as a function of temperature. The velocity data are in good agreement with a cubic extrapolation of high-temperature ultrasonic data from [29] (dotted line). The linear fit to the velocity data and the two linear fits for α/f^2 are used to calculate the effective medium plots in figure 5.

4. Conclusion

In conclusion, we have studied the percolative transition of a three-component water-in-oil microemulsion system, AOT–water–decane, by using a heterodyne-detected transient grating set-up. Our measurements, made at exchanged wavevectors $q = 1\,\mu m^{-1}$ and $q = 2\,\mu m^{-1}$, i.e. sound frequencies around 200 and 420 MHz, show a small but clear effect of the percolation transition on the sound propagation. To our
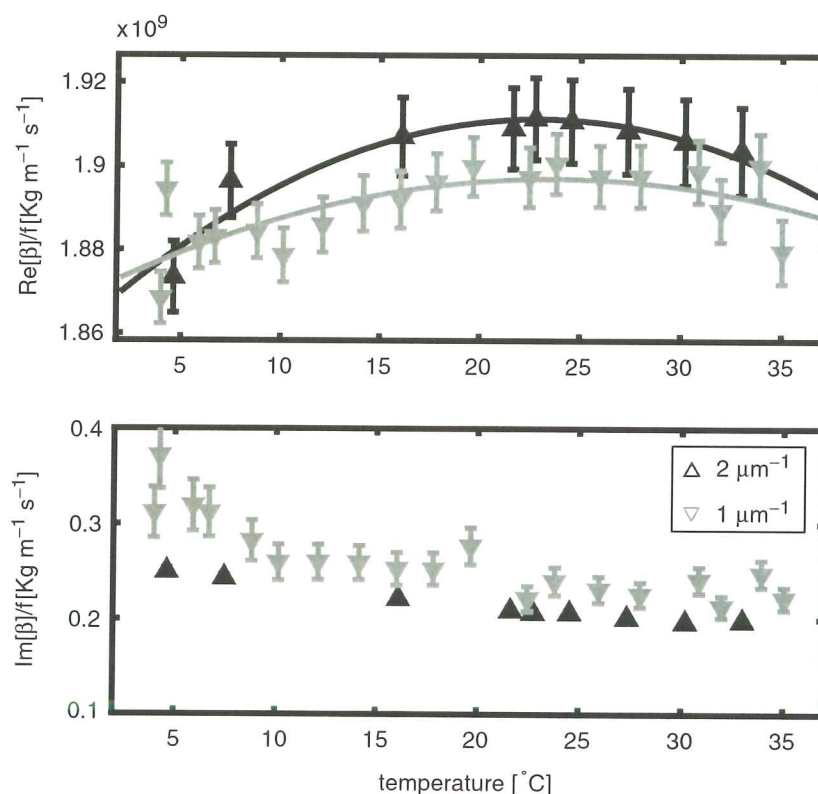
C. Ziparo et al.

Figure 5.   Real and imaginary parts of the elastic modulus of the dispersed phase, calculated in the effective medium approach from the microemulsion and oil sound velocity and sound absorption coefficient, as a function of temperature. The quadratic fits superimposed on $\mathrm{Re}(\beta)$ have maxima for $T = 23.6°\mathrm{C}$ ($q = 1\ \mu m^{-1}$) and $T = 22.9°\mathrm{C}$ ($q = 2\ \mu m^{-1}$), around the percolation temperature observed in the static conductivity [3].

knowledge this is the first time that the percolation transition has been detected by an acoustic measurement in the temperature domain.

Acknowledgments

References

[1] L. Letamendia, E. Pru-Lestret, P. Panizza *et al.*, Physica A **300** 53 (2001).
[2] P. Tartaglia, J. Rouch and S.H. Chen, Phys. Rev. **A 45** 7257 (1992).
[3] C. Cametti, P. Codastefano, G. D'Arrigo *et al.*, Phys. Rev. **A 42** 3421 (1990).

[4] F. Mallamace, N. Micali, C. Vasi *et al.*, Phys. Rev. **A 43** 5710 (1990).

[5] L. Ye, D.A. Weitz, P. Sheng *et al.*, Phys. Rev. **A 44** 8249 (1991).

[6] J. Huang, L. Ye, D. Weitz, P. Sheng *et al.*, Progr. Colloid Polym. Sci. **81** 70 (1990).

[7] L. Letamendia, E. Louisor, E. Pru-Lestret *et al.*, Colloids and Surfaces **A140** 289 (1998).

[8] L. Ye, D.A. Weitz, P. Sheng *et al.*, Phys. Rev. Lett. **63** 263 (1989).

[9] S.H. Chen, J. Rouch, F. Sciortino *et al.*, J. Phys.: Cond. Matt. **6** 10855 (1994).

[10] S.H. Chen, J. Rouch, and P. Tartaglia, Physica A **204** 134 (1994).

[11] M. Kotlarchyk, E.Y. Sheu, and M. Capel, Phys. Rev. **A46** 928 (1992).

[12] J. Huang, S.A. Safran, M.W. Kim *et al.*, Phys. Rev. Lett. **53** 592 (1984).

[13] A. Di Biasio, C. Cametti, P. Codastefano, *et al.*, Phys. Rev. **E47** 4258 (1993).

[14] J. Rouch, N.M. Ziou, C. Cametti *et al.*, J. Phys.: Cond. Matt. **2** SA353 (1990).

[15] J. Huang, J. Surface Sci. Technol. **5** 83 (1989).

[16] E.Y. Sheu, S.H. Chen, J.S. Huang *et al.*, Phys. Rev. **A39** 5867 (1989).

[17] S.H. Chen and J.S. Huang, Phys. Rev. Lett. **55** 1888 (1985).

[18] C. Cametti, P. Codastefano, P. Tartaglia *et al.*, Phys. Rev. Lett. **64** 1461 (1990).

[19] D. Senatra, R. Pratesi, and L. Pieraccini, J. Therm. Anal. **51** 79 (1998).

[20] P.L. Luisi, P. Meier, V.E. Imre *et al.*, Enzymes and nucleic acids in hydrocarbon solvents with the help of reverse micelles, in *Reverse Micelles*, edited by P.L. Luisi and B.E. Straub (Plenum, New York, 1984).

[21] R. Torre, A. Taschin, and M. Sampoli, Phys. Rev. **E64** 061504 (2001).

[22] Y.-X. Yan and K.A. Nelson, J. Chem. Phys. **87** 6240 (1987).

[23] R. Torre, *Time Resolved Spectroscopy in Complex Liquids* (Springer, New York), in press.

[24] G. Goodno, G. Dadusc, and R.D. Miller, J. Opt. Soc. Am. B **15** 1791 (1998).

[25] A.A. Maznev, K.A. Nelson, and J.A. Rogers, Opt. Lett. **23** 1319 (1998).

[26] C.L. O'Connor and J.P. Schlupf, J. Chem. Phys. **47** 31 (1967).

[27] National Institute of Standards and Technology, http://webbook.nist.gov

[28] A. Taschin, P. Bartolini, M. Ricci *et al.*, Phil. Mag. **84** 1471 (2004).

[29] T.S. Khasanshin and A.P. Shchemelev, High Temp. **39** 60 (2001).